WU B 10-36

The form factors for the photon to pseudoscalar meson transitions - an update

P. Kroll

Fachbereich Physik, Universität Wuppertal, 42097 Wuppertal, Germany
and
Institut für Theoretische Physik, Universität Regensburg,
93040 Regensburg, Germany

Abstract

The form factors for the transitions $\pi\gamma$, $\eta\gamma$, $\eta'\gamma$ and $\eta_c\gamma$ are analyzed within the modified perturbative approach in which quark transverse degrees of freedom are retained. The results for the form factors are compared to experiment in detail. As compared to previous calculations within the same approach only little modifications of the meson distribution amplitudes are required in general in order to achieve agreement with experiment. Only for the $\pi\gamma$ form factor a strong contribution from the second Gegenbauer term is found. It also commented on the case of two virtual photons and on the transition form factors in the time-like region.

December, 12 2010

1 Introduction

The simplest exclusive observable is the $\pi\gamma$ transition form factor, $F_{\pi\gamma}$. It has been shown [1] that its behavior for large photon virtuality, Q^2, is determined by the operator product expansion of the product of two electromagnetic currents near the light cone. The only soft physics information required in the calculation of the form factor is the pion wave function. It is however theoretically not understood what large Q^2 means or, in other words, at

which value of Q^2 this collinear factorization approach can be applied. This is still to be decided by comparison with experiment.

In 1995 the CLEO collaboration [2] showed the first data on the $\pi\gamma$ transition form factor at fairly large values of Q^2, actually up to 8 GeV^2. These data provoked an enormous theoretical activity. It seemed that collinear QCD provides a large contribution to the transition form factor. The data lie only about 20% below the asymptotic limit of that form factor, namely $Q^2 F_{\pi\gamma} \to \sqrt{2} f_\pi$ where f_π (= 131 MeV) is the pion's decay constant. Next-to-leading order (NLO) corrections [3] account for about a half of the difference between the asymptotic results and the data. For the remaining difference several explanations were proposed: a pion distribution amplitude slightly different from the asymptotic one ($\Phi_{AS} = 6x(1-x)$), low renormalization scales which enhance the NLO corrections, power corrections or quark transverse momenta to mention a few mechanisms. Since all these mechanisms have to provide only little effects the $\pi\gamma$ transition form factor was believed to be the theoretically best understood exclusive observable.

Recently, this believe has been ruined. The BaBar collaboration [4] has measured the $\pi\gamma$ transition form factors up to about 35 GeV^2. While these data agree with the CLEO data [2, 5] below 8 GeV^2 they reveal an expectedly large rise towards large Q^2. This behavior is in dramatic conflict with dimensional scaling and turned previous calculations obsolete. As the CLEO data in 1995 the BaBar data renewed the interest in this quantity and many paper papers have already been devoted to its theoretical analysis, e.g. [6] - [13].

Here, in this article, it is proposed to employ the modified perturbative approach (MPA) invented by Sterman and collaborators [14, 15]. This approach which bases on $\mathbf{k}_\perp$ factorization, has been used before in the analysis of the CLEO data [16, 17]. It will be shown below that a good fit to the BaBar data can be achieved with this approach, only a few higher order terms in the Gegenbauer representation of the distribution amplitudes have to be taken into account now. Arguments will also be given why in the Q^2 range covered by the CLEO data the simple asymptotic distribution amplitude suffices for a fair fit to the data. In the next section the MPA will be described in some detail and its properties discussed. Next, in Sect. 3, the actual analysis of the data on the $\pi\gamma$ form factor will be presented and the results compared with other theoretical approaches. Sect. 4 is devoted to the analysis of the $\eta\gamma$ and $\eta'\gamma$ transition form factors which have been measured by CLEO [5] and the L3 collaboration [18] previously and by BaBar [19] recently. The Babar

data [20] on the $\eta_c\gamma$ transition form factor will be analyzed in Sect. 5 briefly. Comments on the case of two virtual photons and on the form factors in the time-like region will be presented in the respective Sects. 6 and 7 before the papers ends with a summary (Sect. 8). Details of the Sudakov factor will be presented in an Appendix.

2 The modified perturbative approach

An alternative to the usual collinear factorization is the transverse-momentum ($\mathbf{k}_\perp$)-factorization. For hard exclusive processes this type of factorization has been proposed by Sterman and collaborators [14, 15]. Further arguments for the validity of $\mathbf{k}_\perp$-factorization are given in [21] for the case of the transition form factors. Nevertheless a rigorous proof of $\mathbf{k}_\perp$-factorization does not exist as yet. The basic idea of $\mathbf{k}_\perp$-factorization is to retain the quark transverse degrees of freedom in the hard scattering. This however implies that quarks and antiquarks are pulled apart in the transverse-configuration or impact-parameter space. The separation of color sources is accompanied by the radiation of gluons. Based on previous work by Collins *et al* [22, 23, 24] the corrections to the hard scattering process due to gluon radiation have been calculated in Ref. [14] in axial gauge using resummation techniques and having recourse to the renormalization group. These radiative corrections comprising re-summed leading and next-to-leading logarithms which are not taken into account by the usual QCD evolution, are presented in the form of a Sudakov factor in the impact-parameter plane.

The $\mathbf{k}_\perp$-factorization combined with a Sudakov factor is termed the MPA. Its advantage is that the end-point regions where one of the parton momentum fractions tends to zero, are strongly damped. Large contributions to the form factor accumulated in the soft end-point regions would render the use of perturbation theory inconsistent. As has been pointed out by Isgur and Llewellyn-Smith [25] this is frequently the case in collinear factorization at experimentally accessible values of momentum transfer, typically a few GeV^2. Another advantage of the MPA is that the renormalization scale, μ_R, can be chosen to be momentum-fraction dependent in order to eliminate large logarithms from higher-order perturbative corrections. Eventual α_s-singularities are canceled by the Sudakov factor without introducing additional *ad hoc* cut-off parameters as for instance a parton mass. Thus, the MPA provides well-defined expressions for form factors and amplitudes of

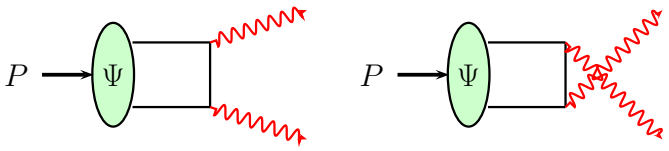

Figure 1: Lowest order Feynman graphs for the $P\gamma$ transition form factor.

hard scattering processes: the perturbative contributions can be calculated in a self-consistent way, even for momentum transfers as low as a few GeV^2.

According to [16, 17] the form factor for a transition from a photon to a pseudoscalar meson (P) reads

$$F_{P\gamma}(Q^2) \;=\; \int dx \frac{d^2\mathbf{b}}{4\pi}\, \hat{\Psi}_P(x,-\mathbf{b},\mu_F)\hat{T}_H^P(x,\mathbf{b},Q,\mu_R)e^{-S(x,b,Q,\mu_R,\mu_F)}\,, \qquad (1)$$

within the MPA. Since the Sudakov exponent S is given in the impact-parameter ($\mathbf{b}$) space, see App. A, it is convenient to work in that space which is canonically conjugated to the $\mathbf{k}_\perp$-space. In the convolution formula (1) $\hat{T}_H$ is the Fourier transform of the momentum-space hard scattering amplitude T_H evaluated to lowest order perturbative QCD from the Feynman graphs displayed in Fig. 1 but taking into account quark transverse momenta

$$T_H^P \;=\; \frac{4\sqrt{6}\,C_P}{xQ^2+\mathbf{k}_\perp^2}\,, \qquad (2)$$

Here C_P is a charge factor. For instance, for the pion it reads $C_\pi = (e_u^2 - e_d^2)/\sqrt{2}$ where e_a denotes the charge of a flavor-a quark in units of the positron charge. The Fourier transform of (2) is

$$\hat{T}_H^P \;=\; \frac{2\sqrt{6}\,C_P}{\pi}\, K_0(\sqrt{x}Qb)\,, \qquad (3)$$

where the Fourier transform is defined by

$$\hat{f}(\mathbf{b}) \;=\; \frac{1}{(2\pi)^2}\int d^2\mathbf{k}_\perp \exp\left[-i\,\mathbf{b}\cdot\mathbf{k}_\perp\right] f(\mathbf{k}_\perp)\,. \qquad (4)$$

The function K_0 denotes the modified Bessel function of order zero.

Another item in (1) is $\hat{\Psi}_P$, the light-cone wave function of the meson P in the impact-parameter space. In the original version of the MPA [15] this

wave function is assumed to be just the meson distribution amplitude Φ_P. As argued in [15] the Sudakov factor e^{-S} can be viewed as the perturbatively generated transverse part of the wave function. For low and intermediate values of Q^2, however, the non-perturbative intrinsic $\mathbf{b}$- or $\mathbf{k}_\perp$-dependence of the light-cone wave function cannot be ignored as has been pointed out in [26]. The inclusion of the transverse size of the meson extends considerably the region in which the perturbative contribution to the form factor can be calculated. As in [17, 26] the wave function is parameterized in the form

$$\hat{\Psi}_P(x,\mathbf{b},\mu_F) \;=\; 2\pi\frac{f_P}{\sqrt{6}}\,\Phi_P(x,\mu_F)\,\exp\Big[-\frac{x\bar{x}b^2}{4\sigma_P^2}\Big]\,. \tag{5}$$

The distribution amplitude, Φ_P, possesses a Gegenbauer expansion

$$\Phi_P(x,\mu_F) \;=\; \Phi_{\rm AS}\left[1+\sum_{n=2,4,\cdots} a_n(\mu_0)\Big(\frac{\alpha_{\rm s}(\mu_F)}{\alpha_{\rm s}(\mu_0)}\Big)^{\gamma_n} C_n^{3/2}(2x-1)\right], \tag{6}$$

where the evolution of the expansion parameters a_n from an initial scale, μ_0, to the factorization scale, μ_F, is controlled by the anomalous dimensions ($n\geq 0$)

$$\gamma_{n+2} \;=\; \gamma_n + 4\frac{C_F}{\beta_0}\frac{(2n+5)(n^2+5n+5)}{(n+1)(n+2)(n+3)(n+4)}\,. \tag{7}$$

Here, $\gamma_0=0$, $C_F=4/3$ and $\beta_0=11-2/3n_f$, n_f is the number of active flavors. For the cases of interest in this work the distribution amplitude is symmetric under the replacement of the momentum fraction x by $\bar{x}=1-x$. This symmetry is already taken into account in (2). The transverse size parameter σ_P being related to the r.m.s transverse momentum by (with $a_0=1$)

$$\begin{aligned}\langle\mathbf{k}_\perp^2\rangle &= \frac{6\pi^2 f_P^2}{P_{q\bar{q}}}\int dx x^2\bar{x}^2\sum_{n=0,2,\cdots}\Big[a_n^2(C_n^{3/2})^2+2a_n a_{n+2}C_n^{3/2}C_{n+2}^{3/2}\Big]\\ &= \frac{\pi^2 f_P^2}{5P_{q\bar{q}}}\Big[1-\frac{6}{7}a_2(1-2a_2)-\frac{150}{77}a_4(a_2-\frac{35}{26}a_4)+\ldots\Big]\end{aligned} \tag{8}$$

For later use the probability of the meson's valence Fock state is also quoted:

$$P_{q\bar{q}} \;=\; \int dx\,\frac{d^2b}{4\pi}\mid\hat{\Psi}_P(x,\mathbf{b})\mid^2 = 3\pi^2 f_P^2\sigma_P^2\sum_{n=0,2,\cdots} a_n^2\,\frac{(n+1)(n+2)}{2n+3}\,. \tag{9}$$

The requirement $P_{q\bar{q}} \leq 1$ leads to bounds on the Gegenbauer coefficients or strictly speaking, on the products $a_n\sigma_P$

$$| \, a_n\sigma_P \, | \leq \frac{1}{\pi f_P} \sqrt{\frac{2n+3}{3(n+1)(n+2)}} \, . \tag{10}$$

For instance, if $\sigma_P = 0.5\,(1.0)$ GeV^{-1} at the initial scale μ_0 one finds

$$a_2(\mu_0) \leq 2.14\,(1.07)\,, \qquad a_4(\mu_0) \leq 1.70\,(0.85)\,. \tag{11}$$

The Sudakov exponent S in (1) which comprises the characteristic double logarithms produced by overlapping collinear and soft divergencies for massless quarks, is given in App. A. The impact parameter $\mathbf{b}$ which represents the transverse separation of quark and antiquark, acts as an infrared (IR) cut-off parameter [1] [22, 23, 24]. Thus, $1/b$ in the Sudakov exponent marks the interface between the non-perturbative soft momenta which are implicitly accounted for in the hadron wave function, and the contributions from soft gluons, incorporated in a perturbative way in the Sudakov factor. Obviously, the IR cut-off serves at the same time as the gliding factorization scale

$$\mu_F \, = \, 1/b \tag{12}$$

to be used in the evolution of the wave function. In accord with this interpretation the entire Sudakov factor is continued to zero whenever $b > 1\Lambda_{\rm QCD}$. In this large-b region the wavelength of the radiative gluon is larger than $1/\Lambda_{\rm QCD}$. Because of the color neutrality of the hadron such gluons cannot resolve the hadron's quark distribution; hence radiation is damped. Soft gluons with wavelength larger than $1/\Lambda_{\rm QCD}$ are therefore to be excluded from perturbation theory; they have to be absorbed into the soft wave function.

Radiative corrections with wavelengths between the IR cut-off and the upper limit $\sqrt{2}/\xi Q$ yield to suppression through the Sudakov factor as is evident from the integration limits in (A.2) (ξ is either x or $1-x$). Gluons with even shorter wavelengths are regarded as hard ones which are considered as higher-order perturbative corrections of the hard scattering and, hence, are not part of the Sudakov factor. For that reason, the Sudakov function

[1] For a more complicated system like the proton's electromagnetic form factor, there are several $\mathbf{b}$'s. In order to cancel the $\alpha_{\rm s}$ singularities the $\mathbf{b}$'s have to be chosen appropriately [27].

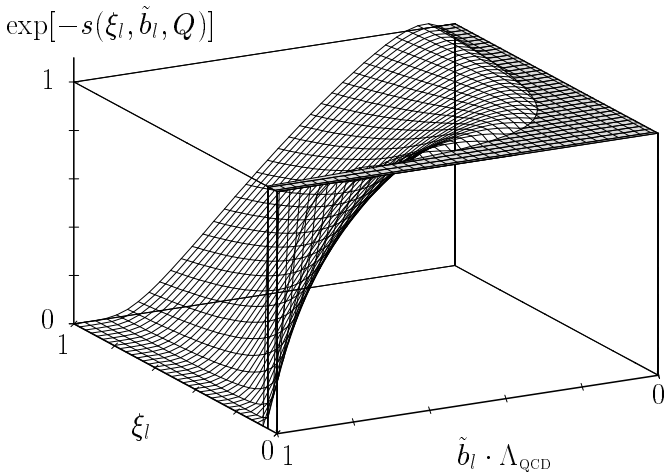

Figure 2: The exponential of the Sudakov function $s(\xi_l, \tilde{b}_l, Q)$ vs $\xi_l = \xi$ and $\tilde{b} = b$ for $Q = 30\Lambda_{\rm QCD}$. The hatched area indicates the hard scattering region. The plot is taken from [27].

$s(\xi, b, Q)$ which is defined in (A.6) and is related to S according to (A.1), is set equal to zero [15] whenever

$$\xi \leq \frac{\sqrt{2}}{Qb}\,. \tag{13}$$

In Fig. 2 the exponential of the Sudakov function $\exp[-s(\xi, b, Q)]$ for $Q = 30\ \Lambda_{\rm QCD}$ is displayed. The properties of the Sudakov function lead to an asymptotic damping of any contribution except those from configurations with small quark-antiquark separations, i.e. for $\ln Q^2 \to \infty$ the limiting behavior of the transition from factors in collinear factorization emerges, for instance, $F_{\pi\gamma} \to \sqrt{2} f_\pi / Q^2$.

In a NLO calculation of the $P\gamma$ form factor or, say, in the case of the electromagnetic pion form factor a momentum-fraction dependent renormalization scale leads to a singular $\alpha_{\rm s}$ in the limit $\mu_R \to \Lambda_{\rm QCD}$. This singularity is canceled in the MPA: whenever $\alpha_{\rm s}$ tends to infinity the Sudakov factor e^{-S} rapidly decreases to zero. As one may suspect from Fig. 2 this does not seem to be the case in the region determined by $b\Lambda_{\rm QCD} \to 1$ and simultaneously $\xi \leq \sqrt{2}\Lambda_{\rm QCD}/Q$, where $\exp[-s(\xi, b, Q)]$ is fixed to unity. However, in this region the other Sudakov function in (A.1), namely $s(1-\xi, b, Q)$, provides

the required suppression. The logarithmic singularities $[\ln(1/(b\Lambda_{\rm QCD})^2]^{-\gamma_n}$ which arise from the evolution of the wave function and which become worse with increasing Gegenbauer index are analogously cancelled by the Sudakov factor.

In analogy to the case of the pion's electromagnetic form factor [15] the maximum of the longitudinal scale appearing in the scattering amplitude (2) and the transverse scale

$$\mu_R \,=\, \max(\sqrt{x}Q, 1/b)\,, \tag{14}$$

is chosen as the renormalization scale [16, 17]. Although to lowest order there is no $\alpha_{\rm s}$ in the hard scattering amplitude for the $P\gamma$ transition form factor, it nevertheless depends on μ_R. Indeed, as discussed above, the Sudakov factor comprises the gluonic radiative corrections for scales between $1/b$ and $\xi Q/\sqrt{2}$. Hence, the latter scale specifies the onset of the hard scattering regime.

Inserting the Gegenbauer decomposition (6) of the meson distribution amplitude into (1) and integrating term by term one can write the $P\gamma$ transition form factor as

$$Q^2 F_{P\gamma} \,=\, 6 C_P f_P \sum_{n=0,2,4\ldots} a_n(\mu_0)\, \mathcal{C}_n(Q^2, \mu_0, \sigma_P) \tag{15}$$

The functions $\mathcal{C}_n$ incorporate the integrals over the product of the n-th Gegenbauer component of the meson wave function, the hard scattering amplitude and the Sudakov factor as well as the change of the Gegenbauer coefficients with the factorization scale. The evolution is worked out with the 1-loop expression for $\alpha_{\rm s}$ using $\Lambda_{\rm QCD} = 0.181$ GeV and four flavors. This value of $\Lambda_{\rm QCD}$ is used throughout the paper except stated otherwise. In (15) μ_0 merely acts as the scale at which the Gegenbauer coefficients of the distribution amplitude are quoted; the transition form factor is independent of it. Numerical results for the ratios $\mathcal{C}_n/\mathcal{C}_0$ obtained under neglect of the intrinsic transverse momentum (i.e. for $\sigma_P \to \infty$), are shown in Fig. 3. A remarkable property of the MPA is to be observed from this figure: For $n > 0$ and low Q^2 the Gegenbauer terms $\mathcal{C}_n$ are suppressed as compared to the lowest one, $\mathcal{C}_0$. The strength of the suppression grows with the Gegenbauer index. A closer inspection of the functions $\mathcal{C}_n$ in (15) reveals that the Sudakov factor in conjunction with the hard scattering amplitude provides a series of power suppressed terms which come from the region of soft quark momenta

$(x, 1-x \to 0)$ and grow with the Gegenbauer index [28]. With increasing Q^2 the higher Gegenbauer terms become gradually more important. At very large Q^2 however the evolution of the expansion coefficients again suppresses all $\mathcal{C}_n$ except $\mathcal{C}_0$. Asymptotically, one has $\mathcal{C}_0 = 1$ and $\mathcal{C}_n = 0$ for $n > 0$ and the asymptotic limit of the transition form factor emerges. The behavior of the $\mathcal{C}_n$ in the MPA is very different from that in the collinear factorization approach. To LO for instance one has

$$\mathcal{C}_0^{\rm coll} \,=\, 1\,, \qquad \mathcal{C}_n^{\rm coll} \,=\, [\alpha_{\rm s}(\mu_F)/\alpha_{\rm s}(\mu_0)]^{\gamma_n}\,. \tag{16}$$

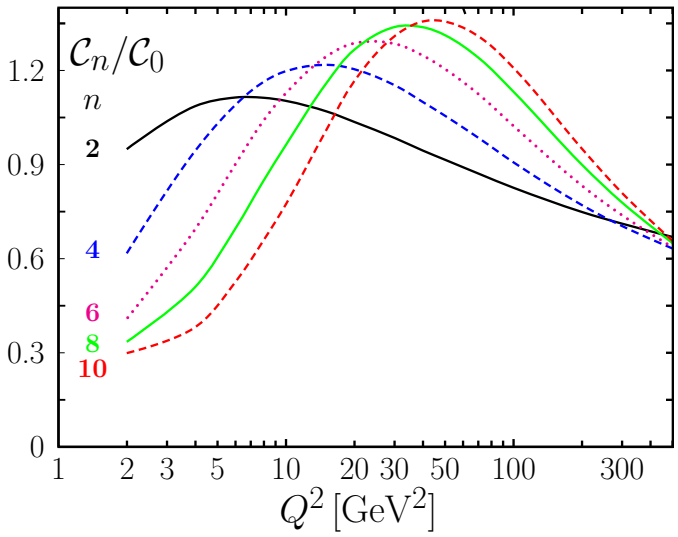

Figure 3: The relative strength of the contributions from the n-th Gegenbauer term to the $P\gamma$ form factor, scaled by the $n = 0$ term, at the scale 1.0 GeV. Intrinsic $\mathbf{k}_\perp$ is omitted. (Colors online)

The intrinsic transverse momentum dependence of the wave function, on the other hand, also provides a series of power suppressed terms but these come from all x and do not grow with n [28]. These power corrections superimposes those generated by the Sudakov factor in combination with the hard scattering amplitude. For small values of the parameter σ_P the power corrections from the intrinsic transverse momentum dependence are rather strong and weaken the relative supppression of the higher Gegenbauer terms,

in particular for small n. In exchange for this the $\mathcal{C}_0$ term itself increases more sharply with rising Q^2 towards the asymptotic limit $\mathcal{C}_0 = 1$.

This property of the MPA explains why the CLEO data on the $\pi\gamma$ transition form factor [5] are well described by the asymptotic distribution amplitude as shown in [17] (with $\sigma_\pi = 0.861\ \text{GeV}^{-1}$, $\Lambda_{\rm QCD} = 0.20\ \text{MeV}$), see Fig. 4. With the BaBar data [4] at disposal which extend to much larger values of Q^2 and do exceed the asymptotic limit $\sqrt{2}f_\pi$, higher Gegenbauer terms can no more be ignored; they are now required for a successful description of the transition form factors. What can be learned about the higher Gegenbauer terms from the BaBar data will be discussed in the next sections.

3 Confronting with the BaBar data on $\pi\gamma$ transitions

Now, having specified all details of the MPA, one can analyze the $\pi\gamma$ form factor by inserting (5) and (6) into (1) and fitting the Gegenbauer coefficients to the CLEO [5] and BaBar [4] data. From a detailed examination of the data it becomes apparent that besides the transverse size parameter only one Gegenbauer coefficient can safely be determined. If more coefficients are freed the fits become unstable. The coefficients acquire unphysically large absolute values between 1 and 10 (often in conflict with the bound (10)) and with alternating signs leading to strong compensations among the various terms. The reason for this fact is that the data show the tendency of a sharp increase of the slope in the vicinity of $Q^2 \simeq 10\ \text{GeV}^2$ while theory for $a_n > 0$ provides a slowly decreasing slope. With large absolute values and alternating signs of the coefficients a slightly increasing slope is produced for a finite range of Q^2.

Two fits are ultimately performed: for the first one the Gegenbauer coefficient a_2 is fitted; for the second one a_4 is freed but a_2 is fixed at the face result of a recent lattice QCD calculation [29]. Evolved to the scale $\mu_0 = 2\ \text{GeV}$ with $\Lambda_{\rm QCD} = 181\ \text{MeV}$, the lattice result [29] is $a_2(\mu_0) = 0.201 \pm 0.114$. All other Gegenbauer coefficients are assumed to be negligible in the fits. The results of the two fits are [2]

$$\sigma_\pi \,=\, 0.40 \pm 0.06\ \text{GeV}^{-1}\,, \qquad a_2(\mu_0) \,=\, 0.22 \pm 0.06\,, \quad \chi^2 = 34.1\,, \quad (17)$$

[2]The Gegenbauer coefficient a_n at a scale μ_1 is obtained from the value quoted in (17) or (18) by multiplying it with the factor $[\ln(\mu_0^2/\Lambda_{\rm QCD}^2)/\ln(\mu_1^2/\Lambda_{\rm QCD}^2)]^{\gamma_n}$.

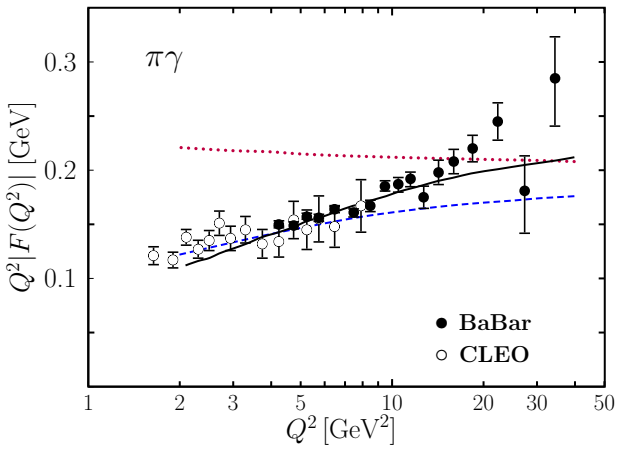

Figure 4: The scaled $\pi\gamma$ transition form factor versus Q^2 evaluated from fit (18) (solid line). The dashed line represents the result given in [17] which is obtained from the asymptotic distribution amplitude and $\sigma_\pi = 0.861$ GeV^{-1} given. The dotted line is obtained from collinear factorization to NLO accuracy. Data taken from [4, 5]. (Colors online)

and with $a_2(\mu_0) = 0.20$ [29],

$$\sigma_\pi \;=\; 0.40 \pm 0.06 \;\text{ GeV}^{-1}\,, \qquad a_4(\mu_0) \;=\; 0.01 \pm 0.06\,, \quad \chi^2 = 34.2\,, \quad (18)$$

The fits are stable and have a sharp χ^2 minimum. The minimal values of χ^2 for the two fits are reasonable given that 28 data points for $Q^2 > 2.3$ GeV^2 are included in the fits. The fit (17) yields a value for a_2 that is in good agreement with the lattice result [29] within errors. The fit (18) is shown in Fig. 4; the fit (17) is practically indistinguishable from (18). At the largest values of Q^2 the resultant form factor seems to be a bit small as compared to the BaBar data. Partially responsible for this fact are the large fluctuations the BaBar data exhibit; the fit compromises between all the data. At very large values of Q^2, not shown in Fig. 4, the theoretical result for the form factor, scaled by Q^2, flattens off with a broad maximum at about 200 GeV^2 and decreases subsequently towards its asymptotic value of $\sqrt{2}f_\pi$. The reason for the small value of σ_π in the present fits can easily be understood. The $\mathcal{C}_2$ and $\mathcal{C}_4$ terms demanded by the BaBar data [4] at large Q^2, also contribute at low Q^2, although to a lesser extent. Therefore, the $\mathcal{C}_0$-term with $\sigma_\pi = 0.861$ GeV^{-1}

which fits nicely the low Q^2 data, see Fig. 4, is to be reduced. The only parameter available for this is however σ_π.

In Ref. [30] it is argued that the decay $\pi^0 \to \gamma\gamma$ fixes the wave function at $\mathbf{k}_\perp = 0$ integrated over x. For the wave function (5) this constraint can be turned into a result for the transverse size parameter [31]

$$\sigma_\pi \;=\; \Big[8\pi^2 f_\pi^2 \sum_{n=0,2,4\ldots} a_n\Big]^{-1/2}. \tag{19}$$

For the asymptotic distribution amplitude this constraint leads to the value $\sigma_\pi = 0.861\ \text{GeV}^{-1}$ used in [17]. The parameters given in (17), (18) violate (19) plainly. Since it is however unclear at which scale the constraint (19) holds the significance of this violation cannot be judged.

Also shown in Fig. 4 is a typical result of the collinear factorization approach to NLO accuracy (taking $\mu_F = \mu_R = Q$ and, as an example, the Gegenbauer coefficients of the fit (18)). Apparently the shape of that result is in conflict with experiment. A change of the values of the Gegenbauer coefficients or the addition of further coefficients with the proviso that large negative coefficients are excluded, does not alter the shape but only the absolute value of the form factor. Thus, the $\pi\gamma$ transition form factor sets an example of a simple exclusive observable for which collinear factorization is insufficient for Q^2 as large as $40\ \text{GeV}^2$.

It is perhaps of interest to examine the role of the soft intrinsic transverse momentum or b-dependence of the wave function further. Thus, one may wonder whether or not a possible scale dependence of the transverse-size parameter improves the fit. This scale dependence has been investigated in [32] and found that σ_π slowly decreases with increasing Q^2. Employing the numerical results given in [32] in the fit, one obtains results for the form factor that are very similar to the ones presented in Fig. 4. As in most applications of light-cone wave functions an approximately scale independent transverse-size parameter is therefore assumed in this work for convenience. If the transverse-size dependence in (5) is neglected which leads to the original version of the MPA [15], a food fit to the form factor data cannot be achieved, the results are too flat as compared to the data and the minimal χ^2 is 155. Hence, the $\mathbf{b}$ dependence of the wave function is an important ingredient of the MPA as has been suggested in [26]. A b-dependence of the wave function like

$$\hat{\Psi}_P \propto \exp\left[-\mathbf{b}^2/4\sigma_\pi^2\right] \tag{20}$$

leads to fits of similar quality as with (5). The obtained values of the Gegenbauer coefficients are slightly larger and have larger errors. Within these errors they however agree with those quoted in (17), (18) within one standard deviation.

One may evaluate the probability (9) of the pion's valence Fock state and the r.m.s. value of $\mathbf{k}_\perp$ (8). From the parameters quoted in (17) and (18) one finds $P_{q\bar{q}} \simeq 0.06$ and $\langle \mathbf{k}_\perp^2 \rangle^{1/2} \simeq 710$ MeV. These values appear to be plausible at a low scale although, in view of the assumption of a scale-independent σ_π, they are to be taken with a grain of salt.

Since the integrations in (1) extend from $x = 0$ to 1 and from $b = 0$ to $1/\Lambda_{\rm QCD}$ the soft regions contribute to the form factor too. The decisive question is how much. In order to investigate this issue a cut-off parameter μ_c is introduced and any contribution to the form factor is set to zero if the renormalization scale (14) is less than μ_c. The accumulation profile is then defined by the ratio $F_{\pi\gamma}(\mu_c)/F_{\pi\gamma}(0)$. It is shown in Fig. 5 and reveals that in the soft regions defined by small values of the renormalization scale (14), say, less than 1 GeV, only small contributions are accumulated. The bulk of the contributions to the transition form factor is generated in regions where the renormalization scale is sufficiently large. Hence, within the MPA, the $\pi\gamma$ transition form factor can be considered as being calculated self-consistently. This property holds down to values of the photon virtuality of about 2 GeV^2.

Li and Mishima [10] also applied the MPA to the $\pi\gamma$ transition form factor and achieved a reasonable fit to the CLEO [5] and BaBar data [4]. In contrast to the present work the flat distribution amplitude [6]

$$\Phi_\pi \equiv 1 \tag{21}$$

is used. It is combined with a Gaussian b-dependence as in (5) in a kind of wave function. However, this product cannot be considered as a proper wave function in so far as it is not normalizable, see (9) [3]. It is furthermore argued in [10] that the distribution amplitude (21) is accompanied by a threshold factor that represents resummed double logs $\alpha_{\rm s} \ln^2 x$ and $\alpha_{\rm s} \ln^2 (1-x)$ arising from the end-point singularities which occur for the flat distribution amplitude in collinear factorization. The threshold factor combined with the flat

[3] The Gegenbauer series of the flat distribution amplitude truncated at n_0 is however normalizable provided n_0 is not too large. Alternatively one may use (20) which leads to a normalizable wave function and provides similar results for the transition form factor if the transverse size parameter is appropriately chosen.

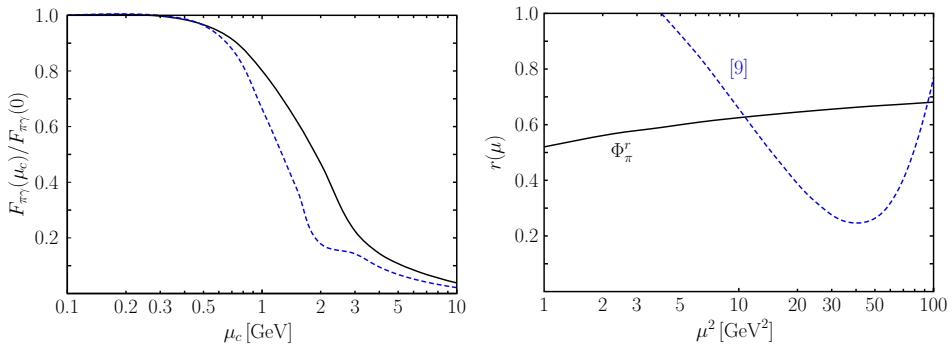

Figure 5: Left: The accumulation profile of the $\pi\gamma$ transition form factor in the space (solid line) and time-like (dashed line) regions versus a cut-off of the renormalization scale at $Q^2 = 10$ GeV^2 evaluated for fit (18). The absolute value of the time-like form factor is displayed. (Colors online). Right: The effective power of the distribution amplitude (22) compared to the power of the threshold factor in [10] at the scale μ.

distribution amplitude can be viewed as an effective distribution amplitude of the type

$$\Phi_\pi^r \;=\; \frac{\Gamma(2+2r)}{\Gamma^2(1+r)}\,[x\bar{x}]^r\,. \tag{22}$$

According to [10], r is about 1 for low Q^2 and small for $Q^2 \simeq 40$ GeV^2. This particular Q^2-dependence of the power r generates the increase of the form factor required by the BaBar data [4]: At low Q^2 the effective distribution amplitude is the asymptotic one implying small values of the transition form factor while, at large Q^2, the effective distribution amplitude is close to the flat one and hence leads to much larger values of the form factor. It is to be stressed that QCD evolution of the proper distribution amplitude, $\Phi_\pi = 1$, is omitted in [10]. Since the gliding factorization scale μ_F is an essential part of the MPA this seems to be a problematic assumption.

Eq. (22) defines a family of power-like distribution amplitudes. It includes the limiting cases of the asymptotic distribution amplitude for $r = 1$ as well as the flat distribution amplitude (21) for $r = 0$. Also the square root distribution amplitude proposed in [33] belongs to this family. By comparison with the Gegenbauer series (6) of (22) and its evolution one can show [28] that the distribution amplitude (22) approximately remains power-like under

evolution, $r \to r(\mu)$ over a large range of the scale.

One may examine the power-like distribution amplitude (22) by fitting the transverse size parameter as well as the power $r(\mu_0)$ to the data on the $\pi\gamma$ form factor. One finds ($\mu_0 = 2$ GeV)

$$\sigma_\pi = 0.40 \pm 0.05 \ \text{GeV}^{-1} \quad r(\mu_0) \ = \ 0.59 \pm 0.06\,, \qquad \chi^2 \ = \ 34.4\,. \tag{23}$$

The quality of this fit to the data on the $\pi\gamma$ form factor is similar to that presented in [10]. In Fig. 5 the power $r(\mu)$ for the fit (23) is compared to the scale dependence of the threshold factor used in [10] (in this work the power is set to unity for $\mu^2 \lesssim 4$ GeV^2). As can be seen from Fig. 5 the distribution amplitude (22) exhibits the usual evolution behavior, it monotonically evolves into the asymptotic one, $\Phi_{\rm AS}$, for $\mu \to \infty$. On the other hand, the scale dependence of the threshold factor or the effective distribution amplitude advocated for in [10], is drastically different. It is also to be stressed that in [10] the threshold factor is evaluated at the scale Q and not at the factorization scale μ_F although it is to be understood as part of the wave function.

The first few Gegenbauer coefficients of the power-like distribution amplitude (23) are compared to those from the fits (17) and (18) in Tab. 1. The first Gegenbauer coefficients of the flat and the square root distribution amplitude advocated for in [33], are also displayed in Tab. 1 for comparison. The comparison is made at a scale of 1 GeV which seems to be a plausible value for soft wave functions like (21). While the Gegenbauer coefficients of the flat distribution amplitude are generally larger than those quoted in (17) or (18), are the coefficients of (23) and the square root distribution amplitude smaller. A wave function like $\Psi = c \exp\left[-\mathbf{b}^2/4\sigma_\pi^2\right]$ to which the flat distribution amplitude is associated, can be used in a MPA calculation without entailing infrared singularities even if evolution is ignored. On the other hand, the use of (21) within the collinear factorization approach leads to an infrared-singular result which necessitates a regularization prescription as for instance the insertion of a mass parameter into the denominator of the quark propagator [7]. Such a regularization prescription typically alters the asymptotic behavior of the scaled form factor drastically: instead of $Q^2\, F_{\pi\gamma} \to$ const. the scaled form factor increases logarithmically [6, 7, 8].

	a_2	a_4	a_6
(17)	0.27 ± 0.07	0	0
(18)	0.25	0.01 ± 0.06	0
(23)	0.14	0.05	0.03
(21)	0.39	0.24	0.18
$\sqrt{x\bar{x}}$	0.15	0.06	0.03

Table 1: Lowest Gegenbauer coefficients for various distribution amplitude at the scale 1 GeV.

4 Generalization to the η and $\eta'\gamma$ form factors

The analysis of the $\pi\gamma$ transition form factor within the MPA can straightforwardedly be extended to the cases of the $\eta\gamma$ and $\eta'\gamma$ ones [34, 35]. These transition form factors may be expressed as a sum of the flavor-octet and flavor-singlet contributions ($P = \eta, \eta'$)

$$F_{P\gamma} \;=\; F^8_{P\gamma} + F^1_{P\gamma}\,. \tag{24}$$

As is the case for the $\pi\gamma$ form factor the functions $F^i_{P\gamma}$ ($i = 1, 8$) are proportional to the constants f^i_P assigned to the decays of meson P through the $\mathrm{SU}(3)_F$ octet or singlet axial-vector weak currents which are defined by the matrix elements

$$\langle 0 \mid J^i_{\mu 5} \mid P(p)\rangle \;=\; i f^i_P\, p_\mu \tag{25}$$

Adopting the general parameterization [36]

$$\begin{aligned} f^8_\eta &= f_8 \cos\theta_8\,, \qquad f^1_\eta \;=\; -f_1 \sin\theta_1\,, \\ f^8_{\eta'} &= f_8 \sin\theta_8\,, \qquad f^1_{\eta'} \;=\; f_1 \cos\theta_1\,, \end{aligned} \tag{26}$$

one can show [37] that on exploiting the divergences of the axial-vector currents - which embody the axial-vector anomaly - the mixing angles, θ_8 and θ_1, differ considerably from each other and from the state mixing angle, θ. In [37] the mixing parameters have been determined:

$$\begin{aligned} f_8 &= 1.26\, f_\pi\,, \qquad f_1 \;=\; 1.17\, f_\pi\,, \\ \theta_8 &= -21.2^\circ\,, \qquad \theta_1 \;=\; -9.2^\circ\,. \end{aligned} \tag{27}$$

Assuming particle-independent [34, 37] octet and singlet wave functions, Ψ^8 and Ψ^1 , which are parameterized as in (5) with the respective decay constants f_8 and f_1 instead of f_π, one can cast the transition form factors into the form

$$\begin{aligned} F_{\eta\gamma} &= \cos\theta_8\, F^8 - \sin\theta_1\, F^1 \\ F_{\eta'\gamma} &= \sin\theta_8\, F^8 + \cos\theta_1\, F^1 \,. \end{aligned} \tag{28}$$

The charge factors in (3) read (with $P = 1, 8$)

$$C_8 \,=\, (e_u^2 + e_d^2 - 2e_s^2)/\sqrt{6}\,, \qquad C_1 \,=\, (e_u^2 + e_d^2 + e_s^2)/\sqrt{3}\,. \tag{29}$$

The asymptotic behavior of the form factors is

$$Q^2 F^8 \to \sqrt{\frac{2}{3}} f_8\,, \qquad Q^2 F^1 \to \frac{4}{\sqrt{3}} f_1\,. \tag{30}$$

It is to be noted that the singlet-decay constant is renormalization-scale dependent [36]:

$$\mu \frac{df_1}{d\mu} \,=\, \gamma_A(\mu)\, f_1 \tag{31}$$

where the anomalous dimension is

$$\gamma_A \,=\, -n_f \left(\alpha_{\rm s}(\mu)/\pi\right)^2 \,. \tag{32}$$

Since the anomalous dimension controlling this scale dependence is of order $\alpha_{\rm s}^2$, it leads to tiny effects. In fact, if the value of f_1 quoted in (27) is to be understood as being valid at, say, the scale $\simeq 1$ GeV, its asymptotic value is 13% smaller; over the range of available data it only decreases by less than 2%. The scale dependence of f_1 is therefore discarded for convenience.

It is to be stressed that to NLO of the hard scattering there is also a contribution from the glue-glue Fock component of the mesons to the singlet form factor [38, 39]. In the MPA analysis performed in this work the glue-glue Fock component does not contribute directly but only through the matrix of the anomalous dimensions and the mixing of the singlet quark-antiquark with the glue-glue distribution amplitude. It is assumed here that the Gegenbauer coefficients of the glue-glue distribution amplitude are zero at a low scale of order 1 GeV. Hence, the quark-antiquark distribution amplitude evolves with the eigenvalues $\gamma_n^{(+)}$ of the anomalous dimension matrix [39]. The values

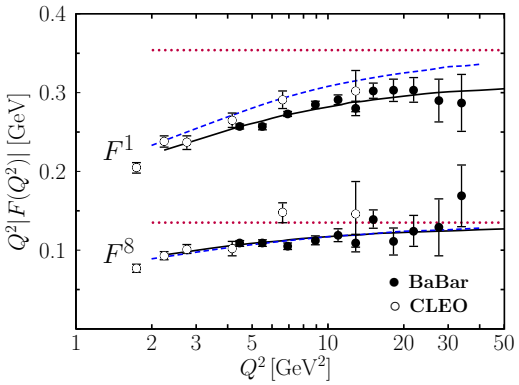

Figure 6: The octet and singlet form factors. Dotted lines represent the asymptotic behavior (30), the dashed lines the results obtained in [34]. The solid lines represent the new fit (33). Data taken from [5, 19]. (Colors online)

of $\gamma_n^{(+)}$ practically fall together with those of γ_n, the anomalous dimension of the octet distribution amplitude, see (7). For instance, $\gamma_2^{(+)} = 0.639$ while $\gamma_2 = 2/3$ for four flavors.

The two form factors F^8 and F^1 can now be evaluated from (1) and (3) in full analogy to the $\pi\gamma$ transition form factor. The data on F^8 and F^1 are extracted from the CLEO [5] and BaBar [19] data using (28). As for the $\pi\gamma$ form factor only the transverse size parameter and one Gegenbauer coefficient for each wave function can be determined. The best fit is obtained with the parameters ($\mu_0 = 2$ GeV):

$$\begin{aligned} \sigma_8 &= 0.84 \pm 0.14 \ \text{GeV}^{-1}, \qquad a_2^8(\mu_0) = -0.06 \pm 0.06, \\ \sigma_1 &= 0.74 \pm 0.05 \ \text{GeV}^{-1}, \qquad a_2^1(\mu_0) = -0.07 \pm 0.04. \end{aligned} \tag{33}$$

The values of χ^2 are 15.0 and 14.1 for the octet and singlet cases, respectively (for 16 data points in each case). The probabilities of the singlet and octet wave functions are 0.24 and 0.19, respectivly. The corresponding r.m.s. $\mathbf{k}_\perp$-values are 390 and 440 MeV.

In Fig. 6 the results of this fit are compared to the data on F^8 and F^1. The quality of this fit is very good. In contrast to the $\pi\gamma$ case the data on both F^8 and F^1 lie below the asymptotic results (30). The combination of these two form factors into the physical ones according to (28) leads to the results which are shown in Fig. 7. Again very good agreement with the data

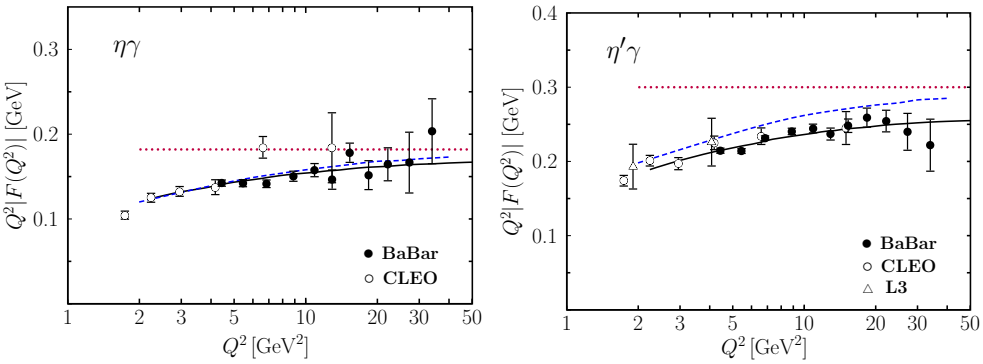

Figure 7: The scaled $\eta\gamma$ and $\eta'\gamma$ transition form factor versus Q^2. Data taken from [5, 18, 19]. For notations refer to Fig. 6. (Colors online)

is to be observed. Also shown in Figs. 6 and 7 are the results obtained in [34] which have been evaluated from the asymptotic distribution amplitudes (with $\sigma_1 = \sigma_8 = 0.861$ GeV^{-1}). The octet as well as the $\eta\gamma$ form factors of [34] are in very good agreement with experiment while the results for F^1 and the $\eta'\gamma$ form factor are somewhat too large.

The form factors scaled by their respective asymptotic behaviors are displayed in Fig. 8. All the form factor ratios for the light mesons behave similar although not identical. Asymptotically they all tend to 1. The $\pi\gamma$ form factor approaches 1 from above, the other ones from below. The approach to 1 is a very slow process; even at 500 GeV^2 the limiting behavior has not yet been reached. It is also evident from Fig. 8 that, forced by the BaBar data, there are strong violations of SU(3)$_F$ flavor symmetry in the groundstate octet of the pseudoscalar mesons at large Q^2. The difference between the $\pi\gamma$ and the $\eta\gamma$ or more precisely the $\eta_8\gamma$ form factors is larger than the difference between their respective decay constants. In other processes involving pseudoscalar mesons, e.g. two-photon annihilations into pairs of pseudoscalar mesons [40, 41], such large flavor symmetry violations have not been observed. Below 8 GeV^2, i.e. in the range of the CLEO data, flavor symmetry breaking is much milder. The $\eta_c\gamma$ transition form factor which is also shown in Fig. 8, behaves very different. This form factor will be discussed in the next section.

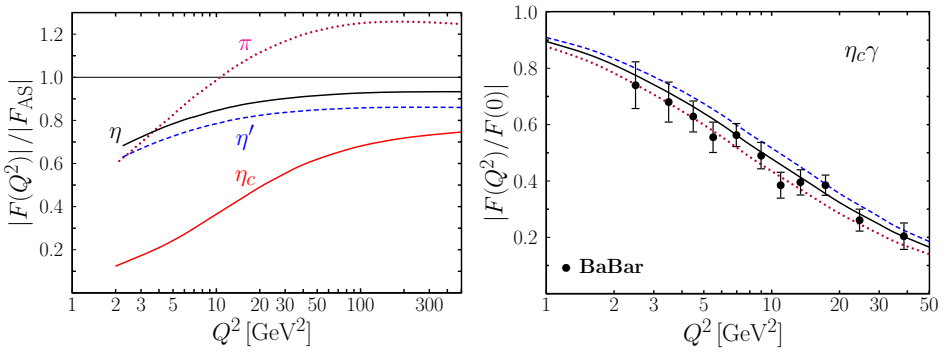

Figure 8: Left: The $P-\gamma$ transition form factors scaled by the corresponding asymptotic behavior, versus Q^2. The thick solid (dashed, dotted, thin solid) line represents the case of the η (η', π, η_c) meson. Parameters are taken from fit (18), (33) and (37). Right: The $\eta_c\gamma$ form factor scaled by its value at $Q^2 = 0$. Data taken from [20]. The solid (dotted) line represents the results of a calculation with the values of the parameters quoted in (37) (with $m_c = 1.26$ GeV). The dashed line is the prediction given in [42]. (Colors online)

5 The case of the η_c

The essential difference of the $\eta_c\gamma$ transition form factor to the other three form factors is the large mass of the η_c (M_{η_c}) or that of the charm quark (m_c). They constitute a second large scale in addition to the virtuality of one of the photons. The masses cannot be neglected in a perturbative calculation in constrast to the case of the light mesons where quark and hadron masses do not play a role. Despite this the $\eta_c\gamma$ form factor is to be calculated from (1) but the hard scattering amplitude to lowest order perturbative QCD reads [42]

$$T_H \;=\; \frac{4\sqrt{6}\,e_c^2}{xQ^2 + (1+4x\bar{x})m_c^2 + \mathbf{k}_\perp^2}\,. \tag{34}$$

The symmetry of the problem under the replacement of x by $\bar{x}$ is already taken into account in (34). Due to the involved second large scale in the problem the $\eta_c\gamma$ form factor can be calculated even at $Q^2 = 0$.

The light-cone wave function of the η_c is parameterized as in (5) [4]. Following [42, 43] the distribution amplitude is chosen as

$$\Phi_{\eta_c} \;=\; N(\sigma_{\eta_c}) x\bar{x} \exp\Big[-\sigma_{\eta_c}^2 M_{\eta_c}^2 \frac{(x-1/2)^2}{x\bar{x}} \Big] \tag{35}$$

where $N(\sigma_{\eta_c})$ is determined from the usual requirement $\int_0^1 dx \Phi_{\eta_c}(x) = 1$. The distribution amplitude exhibits a pronounced maximum at $x = 1/2$ and is exponentially damped in the end-point regions. It describes an essentially non-relativistic $c\bar{c}$ bound state; quark and antiquark approximately share the meson's momentum equally. In the hard scattering amplitude the charm quark mass occurs while in the distribution amplitude the meson mass is used. This property of the latter distribution amplitude is a model assumption which contributes to the theoretical uncertainty of the results. In the sense of the non-relativistic QCD [44] $2m_c$ and M_{η_c} are equivalent. In (1) the Sudakov factor $\exp[-S]$ can be set to 1 in the case at hand for two reasons: First, due to the large, non-negligible c-quark mass the radiative QCD corrections only produce soft divergencies but no collinear ones and, hence, the double logs do not appear. Second, the Sudakov suppressions is mainly active in the end-point regions (c.f. the discussion in Sect. 2) which are already strongly damped by the η_c wave function. The evolution behavior of the η_c distribution amplitude is unknown in the range where Q^2 is of order of $M_{\eta_c}^2$ and is therefore ignored here. Consequently, also the running of the charm quark mass is omitted. It has been checked that the effect of the this scale dependence is anyway only on the percent level.

The normalization of the $\eta_c\gamma$ transition form factor is fixed by its value at $Q^2 = 0$ which is related to two-photon decay width by

$$\Gamma[\eta_c \to \gamma\gamma] \;=\; \frac{1}{4}\,\pi\alpha_{\rm elm}^2\, M_{\eta_c}^3 \;\mid F_{\eta_c\gamma}(0) \mid^2 \;. \tag{36}$$

However, this decay width is experimentally not well known [48]. It is therefore advisable to normalize the form factor by its value at $Q^2 = 0$ all the more so since the recent BaBar data [20] are also presented this way. Doing so the perturbative QCD corrections at $Q^2 = 0$ to the $\eta_c\gamma$ transition form factor which are known to be large [45], are automatically included.

[4] In [42] the Gaussian (20) is taken. The version (5) is chosen here in order to be conform with the calculations of the other form factors. The differences between the two versions are marginal as has been mentioned previously.

Also the α_s corrections for $Q^2 \lesssim M_{\eta_c}^2$ [46] cancel to a high degree in the ratio $F_{\eta_c\gamma}(Q^2)/F_{\eta_c\gamma}(0)$. Even at $Q^2 = 10$ GeV^2 their effect is less than 5%, c.f. the discussion in [42]. The uncertainties in the present knowledge of the η_c decay constant do also not enter the predictions for this ratio.

The recent Babar data on the $\eta_c\gamma$ form factor [20] are shown in the right hand panel of Fig. 8. The behavior of this data has indeed been predicted in [42]. The predictions which have been evaluated from $m_c = M_{\eta_c}/2$, are about one standard deviation too large but with regard to the uncertainties of the theoretical calculation, as for instance the exact value of the mass of the charm quark, one can claim reasonable agreement between theory and experiment. A little readjustment of the value of the charm quark mass improves the fit. Thus, with the parameters

$$m_c = 1.35 \text{ GeV}, \qquad \sigma_{\eta_c} = 0.44 \text{ GeV}^{-1}, \tag{37}$$

a perfect agreement with experiment is achieved as is to be seen in Fig. 8. For comparison there are also shown results evaluated from $m_c = 1.21$ GeV in Fig. 8. As one may note from the left hand panel of Fig. 8 the $\eta_c\gamma$ transition form factor behaves quite differently from the other three form factors. The large charm-quark mass slows down the approach to the asymptotic limit

$$Q^2 F_{\eta_c\gamma} \to \frac{8 f_{\eta_c}}{3}. \tag{38}$$

Finally one may examine whether the parameters quoted in (37) are plausible. For this purpose the $\eta_c\gamma$ form factor at zero momentum transfer is evaluated. Ignoring α_s-corrections as well as relativistic effects and using the value 420 MeV for the η_c decay constant f_{η_c}, one obtains

$$F_{\eta_c\gamma}(0) = 0.085 \text{ GeV}^{-1}, \tag{39}$$

and a two-photon decay width (36) of

$$\Gamma(\eta_c \to \gamma\gamma) = 8.05 \text{ keV}. \tag{40}$$

This result is in good agreement with the value of (7.20 ± 2.11) keV evaluated by the PDG [48] and with recent theoretical estimates, see for instance [47] and references therein. The parameters quoted in (37) together with $f_{\eta_c} = 420$ MeV correspond to a normalization of the η_c distribution amplitude $N(\sigma_{\eta_c}) = 8.849$, to a probability of the valence Fock state of 0.82 and to a r.m.s. $\mathbf{k}_\perp$ of 773 MeV. The latter two values appear reasonable for a quarkonium state.

6 Two virtual photons

An extension of the MPA analysis of the $P\gamma$ transition form factors to the case of two virtual photons can be found in [49, 50, 51]. As an example the $\pi\gamma^*$ form factor will be discussed here. Denoting the photon virtualities by Q^2 and Q'^2 and introducing the variables

$$\overline{Q}^2 \;=\; \frac{1}{2}\,(Q^2+Q'^2)\,, \qquad \omega \;=\; \frac{Q^2-Q'^2}{Q^2+Q'^2}\,, \tag{41}$$

one finds for the hard scattering amplitude the expression

$$\hat{T}_H \;=\; \frac{2}{\sqrt{3}\pi}\,K_0(\sqrt{1-\omega(1-2x)}\,\overline{Q}b) \tag{42}$$

in b-space. In generalization of (1) the $\pi\gamma^*$ form factor now reads

$$F_{\pi\gamma^*}(\overline{Q}^2,\omega) \;=\; \int dx\frac{d^2\mathbf{b}}{4\pi}\,\hat{\Psi}_\pi(x,-\mathbf{b},\mu_F)\hat{T}_H(x,\mathbf{b},\overline{Q},\omega,\mu_R)e^{-S(x,b,\overline{Q},\mu_F,\mu_R)}\,. \tag{43}$$

The renormalization scale is taken as

$$\mu_R \;=\; \max\,(\sqrt{1-\omega(1-2x)}\overline{Q},1/b) \tag{44}$$

in generalization of (14).

The form factor only falls off like $1/\overline{Q}^2$ at large $\overline{Q}^2$ in contrast to the $Q^{-2}Q'^{-2} \propto \bar{Q}^{-4}$ behavior of the vector meson dominance model [52]. It is also interesting to note that like in collinear factorization, the $\pi\gamma^*$ form factor is insensitive to the higher Gegenbauer terms for $Q^2 \simeq Q'^2$; in the limit $\omega \to 0$ it only depends on the asymptotic distribution amplitude. In fact it has been shown [50, 51] that the n-th order Gegenbauer term contributes to order ω^n. The importance of effects from the intrinsic $\mathbf{k}_\perp$ diminishes as both photons become virtual. This is evident from the quark propagator in momentum space reading

$$T_H \propto [(1-\omega(1-2x))\overline{Q}^2+\mathbf{k}_\perp^2]^{-1}\,. \tag{45}$$

As ω deviates from 1, the real photon limit, the form factor $F_{\pi\gamma^*}$ becomes less sensitive to the end-point regions where either the quark or the antiquark becomes soft. In the limit $\omega \to 0$ (45) reduces to $[\overline{Q}^2+\mathbf{k}_\perp^2]^{-1}$. This is to

be contrasted with the $\omega \to 1$ limit in which $T_H \propto [xQ^2 + \mathbf{k}_\perp^2]^{-1}$, see (2). Thus, $\mathbf{k}_\perp$ plays a minor role in the quark propagator provided ω is sufficiently small. In the limit $\omega \to 0$ and large $\overline{Q}^2$ the form factor becomes

$$\overline{Q}^2 F_{\pi\gamma^*}(\overline{Q}^2, \omega) \,=\, \frac{\sqrt{2}}{3} f_\pi \,, \tag{46}$$

a result that has been derived long ago in [53].

The measurement of the space-like $\pi\gamma$ transition form factor is performed in e^+e^- collisions with so-called single-tag events where either the electron or the positron in the final state is detected. This method implies an integration over the spectrum of that exchanged photon which is emitted from the undetected lepton, up to a value of, say, Q'^2 set by an experimental cut. Actually for the BaBar experiment the cut is $Q'^2 < 0.18$ GeV^2. Thus, strictly speaking, one measures the form factor for the transition from a quasi-real photon with an effective virtuality $Q'^2_{\rm eff}$ less than the cut value, to the pion. The question arises how good does this measured form factor approximate the one for the transition from a real photon to the pion. In order to examine this issue $F_{\pi\gamma^*}$ is evaluated for small values of the ratio Q'^2/Q^2 using (43) and the pion wave function parameters from fit (18). As one may see from Fig. 9 where the results for a sample set of Q^2 values are shown, the transition form factor depends on Q'^2 mildly (at least within the MPA) as long as the ratio Q'^2/Q^2 is smaller than about 0.01. At this value of the ratio of the two virtualities the form factor is reduced by about 5% as compared to its value at the real photon limit while at a value of 0.1 of the ratio, the form factor is smaller by about 30%.

7 Remarks on the time-like transition form factors

In the context of the large Q^2 behavior of the transition form factors one may also consider the recent measurement of the time-like $\eta\gamma$ and $\eta'\gamma$ form factors at $s = 112$ GeV^2 by the BaBar collaboration [54]:

$$s|F_{\eta\gamma}| \,=\, 0.229 \pm 0.031 \;\; \text{GeV}\,, \qquad s|F_{\eta'\gamma}| \,=\, 0.251 \pm 0.021 \;\; \text{GeV}\,. \tag{47}$$

Comparing these data with the predictions for the space-like form factors which are shown in Figs. 7 and 8, one notices that for the case of the η the

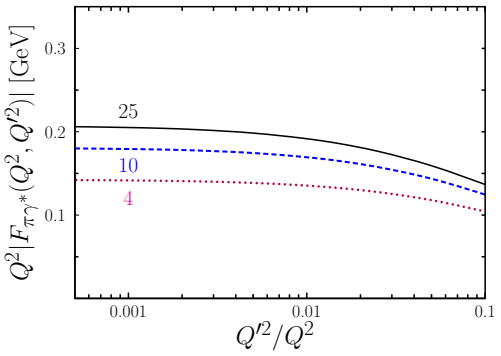

Figure 9: The $\pi\gamma^*$ form factor versus the ratio of the two photon virtualities for $Q^2 = 25\,(10, 4)$ GeV^2 represented as solid (dashed, dotted) line. The parameters of the pion wave function are taken from fit (18). (Colors online)

experimental time-like value is much larger than the predicted space-like one which amounts to 0.169 at $Q^2 = 112$ GeV^2. For the case of the η', on the other hand, the experimental time-like value practically falls together with theoretical result of 0.258 for the space-like form factor.

A detailed study of the pseudoscalar meson-photon transition form factors in the time-like region is beyond the scope of the present article. Within the MPA however, one expects slightly different values for the time-like and space-like transition form factors: The space-like propagator $[xQ^2 + \mathbf{k}_\perp^2]^{-1}$ is to be replaced by $[-xs + \mathbf{k}_\perp^2 - \imath\epsilon]^{-1}$ in the time-like region or, in b-space, $K_0(\sqrt{x}Qb)$ in (3) by $i\pi/2H_0^{(1)}(\sqrt{x}sb)$ with $H_0^{(1)}$ being the zeroth order Hankel function. The pole of the propagator now occurs within the range of integration and in general leads to an enhancement as well as a phase of the form factor. For the case of the electromagnetic form factor of the pion this phenomenon has been pointed out and studied in some detail by Gousset and Pire [55]. The analytic continuation of the Sudakov factor from the space-like to the time-like region, which is necessary too, is not well understood. It probably leads to an oscillating phase [55, 56].

In order to give an admittedly rough estimate of the expected size of the time-like form factor it is followed [55] and the time-like propagator is combined with the space-like Sudakov factor. With this receipe one finds the absolute values 0.25 and 0.24 GeV for the scaled time-like $\pi\gamma$ transition form factor at $s = 3$ and 100 GeV^2, respectively. The corresponding ratios

of the time and space-like transition form factors are $\simeq 1.9$ and $\simeq 1.1$. For s larger than about 5 GeV^2 the time-like form factor is dominantly real, its imaginary part contributes less than about 10% to the absolute value. The accumulation profile of the absolute value of the time-like form factor is displayed in Fig. 5. Although the pole of the propagator occurs in the end-point region (at $\bar{x} = k_\perp/s$) the profile is only mildly softer than that of the space-like form factor, i.e. also the time-like form factor is mainly fed by contributions from regions where the renormalization scale is sufficiently large. In the light of this feature one may consider the results for the time-like transition form factor obtained within the MPA as a tolerable estimate.

Along these lines one can also compute the $\eta\gamma$- and $\eta'\gamma$ transition form factors in the time-like region. Using the parameters quoted in (33) one finds that at $s = 3$ GeV^2 the absolute values of the time-like form factors are about a factor of 2 larger than the space-like form factors. At $s = 112$ GeV^2 the results are $s|F_{\eta\gamma}| \simeq 0.17$ GeV and $s|F_{\eta'\gamma}| \simeq 0.28$ GeV. While for the case of the η' there is rough agreement with experiment (47) within errors, is the $\eta\gamma$ form factor too small by about two standard deviations.

8 Concluding remarks

In this paper an analysis of the form factors for the transitions from a photon to a pseudoscalar meson is presented. The analysis is performed within the MPA which bases on $\mathbf{k}_\perp$ factorization. It is shown that due to the Sudakov suppressions which are an important ingredient of the MPA and which represents radiative corrections in next-to-leading-log approximation summed to all orders of perturbation theory, higher order Gegenbauer terms of the meson's distribution amplitude are suppressed at low Q^2. In fact, the combined effect of the hard scattering kernel and the Sudakov factor leads to a series of power suppressed terms which stem from the soft regions. The intrinsic $\mathbf{k}_\perp$-dependence generates a second series of power corrections which in contrast to the first series, do not grow with the Gegenbauer index. The interplay of these two ingredients results in a remarkable feature of the MPA - the transition form factors are only affected by the few lowest Gegenbauer terms of the distribution amplitude, the higher ones do practically not contribute. How many Gegenbauer terms are relevant depends on the range of Q^2 considered: In the Q^2 range covered by the CLEO data [5] (< 10 GeV^2) it suffices to use just the asymptotic distribution amplitude in order to fit the CLEO

data. With the BaBar data [4, 19] at disposal, covering the unprecedented large range 4 $\text{GeV}^2 < Q^2 < 35$ GeV^2, the next or the next two Gegenbauer terms have to be taken into account or, turning the argument around, can be determined from an analysis of the data on the transition form factors. Indeed this is what has been done in this work. From the present analysis it turns out that for the case of the pion a fairly strong contribution from a_2 is required by the data while for the η and η' much smaller deviations from the asymptotic distribution amplitude are needed. For these cases the results from a previous calculation within the MPA [34] are already in fair agreement with the BaBar data, nearly perfect for the η, slightly worse for the η'. Comparing the $\pi\gamma$ form factor with the $\eta\gamma$ or more precisely the $\eta_8\gamma$ one, one observes a strong breaking of flavor symmetry in the ground-state octet of the pseudoscalar mesons. The difference between the two form factors is larger than the respective decay constants. In other processes involving pseudoscalar mesons such large flavor symmetry violations have not been observed. With regard to the theoretical importance of the transition form factors, in particular the role of collinear factorization a remeasurment, e.g. by the BELLE collaboration, would be highly welcome.

One may wonder what the implications of the new distribution amplitudes for the pseudoscalar mesons are for other hard exclusive processes. A detailed investigation of this issue is beyond the scope of the present paper. It has however been checked that for the pion's electromagentic form factor there is no substantial change. The perturbative contribution to it still amounts to only about a third of the experimental value of the form factor which is measured only at low Q^2 [62]. The perturbative contribution is slightly increasing with growing Q^2 now and not as flat as in [26]. In any case for Q^2 less than 10 GeV^2 the differences are marginal.

Acknowledgements It is a pleasure to thank Volodya Braun and Markus Diehl for their interest in this work and numerous valuable comments. Discussions with Vladimir Druzhinin and Andreas Schäfer are also gratefully acknowledged. This work is supported in part by the BMBF, contract number 06RY258.

A Appendix

In this appendix details of the Sudakov factor are presented. The Sudakov exponent S which comprises the characteristic double logarithms produced by overlapping collinear and soft divergencies (for massless quarks) has been calculated in [14]. In axial gauge, $n \cdot A = 0$, these overlaps arise in general from two-particle reducible Feynman graphs where, before the hard interaction, the gluon is exchanged between the quark and antiquark of the meson or emitted from and reabsorbed by either the quark or the antiquark. The Sudakov factor can therefore be analyzed indepedently of the physical process and can be viewed as part of the meson wave function. For the case of interest, only the two-particle reducible graphs occur anyway. As shown in [14] for a quark-antiquark system the Sudakov exponent reads [5]

$$S \;=\; s(x,b,Q) + s(1-x,b,Q) + 2\int_{\mu_F}^{\mu_R} \frac{d\bar{\mu}}{\bar{\mu}}\,\gamma_q(\alpha_{\rm s}(\bar{\mu}))\,. \tag{A.1}$$

The impact parameter $\mathbf{b}$, canonically conjugated to $\mathbf{k}_\perp$, is the spacial separation of quark and antiquark. The Sudakov function $s(\xi,b,Q)$ where ξ is either x or $1-x$, is given by

$$s(\xi,b,Q) \;=\; \frac{1}{2}\int_{C_1/b}^{C_2\xi Q} \frac{d\mu}{\mu}\,\left\{2\ln\Big(\frac{C_2\xi Q}{\mu}\Big)\mathcal{A}(C_1,g(\mu)) + \mathcal{B}(C_1,C_2,g(\mu))\right\}. \tag{A.2}$$

An appropriate choice of the gauge vector n has been made in order to obtain this result. The function $\mathcal{B}$ has been calculated to order $\alpha_{\rm s}$ in the $\overline{\rm MS}$ scheme explicitly. The function $\mathcal{A}$ arises from the use of the renormalization group equation which is applied in order to absorb all the Q^2 dependence into the scale of the coupling constant. It has been calculated to order $\alpha_{\rm s}^2$:

$$\mathcal{A} \;=\; \frac{\alpha_{\rm s}}{\pi}\,A^{(1)} + \Big(\frac{\alpha_{\rm s}}{\pi}\Big)^2 A^{(2)} + \mathcal{O}(\alpha_{\rm s}^3) \tag{A.3}$$

with

$$A^{(1)} \;=\; C_F\,, \qquad A^{(2)} \;=\; \frac{C_F}{2}\left[\frac{67}{6} - \frac{\pi^2}{2} - \frac{5}{9}n_f + \beta_0\ln\left(C_1 e^{\gamma_E}/2\right)\right], \tag{A.4}$$

[5] Musatov and Radyushkin [57] claim that, due to kinematical properties the Sudakov functions should be summed as $s(x,b,Q) + s(\sqrt{\bar{x}},b,Q)$ where it is assumed that the real photon is attached to the antiquark line. Doing so the universality of the wave function (including the Sudakov factor) is broken. This alternative possibility only leads to tiny numerical differences in the form factor. The predictions change by less than 1%.

where γ_E is the Euler constant. The constants C_1 and C_2 are free parameters which may be chosen in such a way that large logarithms from higher orders in the perturbative expansion of $\mathcal{B}$ are avoided. The conventional choice is

$$C_1 \,=\, 1\,, \qquad C_2 \,=\, \sqrt{2}\,. \tag{A.5}$$

Other choices of the C_i have been discussed in [58].

The Sudakov function has been explicitly given in [14] first. Later repetitions of this calculation [59, 60] led to a slightly different result which is quoted here

$$\begin{aligned} s(\xi,b,Q) \;&=\; \frac{2C_F}{\beta_0}\,\left[\hat{q}\ln\Big(\frac{\hat{q}}{\hat{b}}\Big)-\hat{q}+\hat{b}\right] \\ &+\; \frac{C_F\beta_1}{\beta_0^3}\,\left[\hat{q}\Big(\frac{\ln(2\hat{q})+1}{\hat{q}}-\frac{\ln(2\hat{b})+1}{\hat{b}}\Big)+\frac{1}{2}\ln^2(2\hat{q})-\frac{1}{2}\ln^2(2\hat{b})\right] \\ &+\; 4\frac{A^{(2)}}{\beta_0^2}\,\left[\frac{\hat{q}-\hat{b}}{\hat{b}}-\ln\Big(\frac{\hat{q}}{\hat{b}}\Big)\right]+\frac{C_F}{\beta_0}\ln\Big(\frac{C_1^2e^{2\gamma_E-1}}{C_2^2}\Big)\,\ln\Big(\frac{\hat{q}}{\hat{b}}\Big)\,. \end{aligned} \tag{A.6}$$

The variables $\hat{q}$ and $\hat{b}$ are defined by

$$\hat{q} \,=\, \ln\Big(\frac{C_2\xi Q}{2\Lambda_{\rm QCD}}\Big)\,, \qquad \hat{b} \,=\, \ln\Big(\frac{C_1}{b\Lambda_{\rm QCD}}\Big)\,. \tag{A.7}$$

The last term in (A.6) represents the integrated function $\mathcal{B}$. The differences between the various results for s used earlier [14, 15, 26] and (A.6) are numerically small, of the order of a few percent. It should be noted that the last term in (A.6) is twice as large as in [58]. Also this discrepancy has little effect on the form factor.

The integral in (A.1) arises from the application of the renormalization group equation. It combines the effects of the renormalization group equation on the wave function (with the factorization scale μ_F) and on the hard scattering amplitude involving the renormalization scale μ_R. The evolution from one scale to another is controlled by the anomalous dimension of the quark's wave function in axial gauge [61] $\gamma_q = -\alpha_{\rm s}/\pi \,+\, \mathcal{O}(\alpha_{\rm s}^2)$. It leads to

$$\int_{\mu_F}^{\mu_R}\frac{d\bar{\mu}}{\bar{\mu}}\,\gamma_q(\alpha_{\rm s}(\bar{\mu})) \,=\, \frac{2}{\beta_0}\,\ln\frac{\ln(\mu_F^2/\Lambda_{\rm QCD}^2)}{\ln(\mu_R^2/\Lambda_{\rm QCD}^2)} \tag{A.8}$$

with the help of the 1-loop result for $\alpha_{\rm s}$. Its use is consistent with the derivation of (A.6). In particular the terms in the first line of (A.6) are calculated from the 1-loop $\alpha_{\rm s}$ and these terms dominate the Sudakov function.

References

[1] G. P. Lepage and S. J. Brodsky, Phys. Lett. B **87**, 359 (1979).

[2] V. Savinov *et al* [CLEO collaboration], proceedings of the PHOTON95 workshop, Sheffield (1995), eds. D. J. Miller *et al*, World Scientific.

[3] F. del Aguila and M. K. Chase, Nucl. Phys. B **193**, 517 (1981); E. Braaten, Phys. Rev. D **28**, 524 (1983).

[4] B. Aubert *et al.* [The BABAR Collaboration], Phys. Rev. D **80**, 052002 (2009) [arXiv:0905.4778 [hep-ex]].

[5] J. Gronberg *et al.* [CLEO Collaboration], Phys. Rev. D **57**, 33 (1998) [arXiv:hep-ex/9707031].

[6] A.V. Radyushkin, Phys. Rev. D **80**, 094009 (2009) [arXiv:0906.0323 [hep-ph]].

[7] M. V. Polyakov, JETP Lett. **90**, 228 (2009) [arXiv:0906.0538 [hep-ph]].

[8] A. E. Dorokhov, arXiv:1003.4693 [hep-ph].

[9] A. P. Bakulev, S. V. Mikhailov and N. G. Stefanis, arXiv:1005.3173 [hep-ph]. S. V. Mikhailov, A. V. Pimikov and N. G. Stefanis, Phys. Rev. D **82**, 054020 (2010) [arXiv:1006.2936 [hep-ph]].

[10] H.-S. Li and S. Mishima, Phys. Rev. D **80**, 074024 (2009) [arXiv:0907.0166 [hep-ph]].

[11] S. Noguera and V. Vento, "The pion transition form factor and the pion distribution amplitude," Eur. Phys. J. A **46**, 197 (2010) [arXiv:1001.3075 [hep-ph]].

[12] H. L. L. Roberts, C. D. Roberts, A. Bashir, L. X. Gutierrez-Guerrero and P. C. Tandy, arXiv:1009.0067 [nucl-th].

[13] Y. N. Klopot, A. G. Oganesian and O. V. Teryaev, arXiv:1009.1120 [hep-ph].

[14] J. Botts and G. Sterman, Nucl. Phys. B **325**, 62 (1989).

[15] H. n. Li and G. Sterman, Nucl. Phys. B **381**, 129 (1992).

[16] R. Jakob, P. Kroll and M. Raulfs, J. Phys. G **22**, 45 (1996) [arXiv:hep-ph/9410304].

[17] P. Kroll and M. Raulfs, Phys. Lett. B **387**, 848 (1996) [arXiv:hep-ph/9605264].

[18] M. Acciarri *et al.* [L3 Collaboration], Phys. Lett. B **418**, 399 (1998).

[19] V. P. Druzhinin, arXiv:1011.6159 [hep-ex].

[20] J. P. Lees *et al.* [The BABAR Collaboration], Phys. Rev. D **81** (2010) 052010 [arXiv:1002.3000 [hep-ex]].

[21] M. Nagashima and H. n. Li, Phys. Rev. D **67**, 034001 (2003) [arXiv:hep-ph/0210173].

[22] J. C. Collins and D. E. Soper, Nucl. Phys. B **193**, 381 (1981) [Erratum-ibid. B **213**, 545 (1983)].

[23] J. C. Collins and D. E. Soper, Nucl. Phys. B **194**, 445 (1982).

[24] J. C. Collins, D. E. Soper and G. Sterman, Nucl. Phys. B **261**, 104 (1985).

[25] N. Isgur and C. H. Llewellyn Smith, Nucl. Phys. B **317**, 526 (1989).

[26] R. Jakob and P. Kroll, Phys. Lett. B **315**, 463 (1993) [Erratum-ibid. B **319**, 545 (1993)] [arXiv:hep-ph/9306259].

[27] J. Bolz, R. Jakob, P. Kroll, M. Bergmann and N. G. Stefanis, Z. Phys. C **66**, 267 (1995) [arXiv:hep-ph/9405340].

[28] V. Braun, M. Diehl and P. Kroll, work in progress.

[29] V.M. Braun *et al* [QCDSF/UKQCD collaboration], Phys. Rev. D **74**, 074501 (2006) [arXiv:hep-lat/0606012].

[30] S. J. Brodsky, T. Huang and G. P. Lepage, Partciles and Fields 2, eds. Z. Capri and A. N. Kamal (Banff Summer Institute, 1983), p. 143.

[31] J. Bolz, P. Kroll and G. A. Schuler, Eur. Phys. J. C **2**, 705 (1998).

[32] C. Vogt, Phys. Rev. D **63**, 034013 (2001) [arXiv:hep-ph/0007277].

[33] S. J. Brodsky and G. F. de Teramond, Phys. Rev. D **77**, 056007 (2008) [arXiv:0707.3859 [hep-ph]].

[34] T. Feldmann and P. Kroll, Eur. Phys. J. C **5**, 327 (1998) [arXiv:hep-ph/9711231].

[35] T. Feldmann and P. Kroll, Phys. Scripta **T99**, 13 (2002) [arXiv:hep-ph/0201044].

[36] H. Leutwyler, Nucl. Phys. Proc. Suppl. **64** (1998) 223 [arXiv:hep-ph/9709408]; R. Kaiser and H. Leutwyler, arXiv:hep-ph/9806336;

[37] T. Feldmann, P. Kroll and B. Stech, Phys. Rev. D **58**, 114006 (1998) [arXiv:hep-ph/9802409].

[38] M. A. Shifman and M. I. Vysotsky, Nucl. Phys. B**186**, 475 (1981); V. N. Baier and A. G. Grozin, Nucl. Phys. B**192**, 476 (1981).

[39] P. Kroll and K. Passek-Kumericki, Phys. Rev. D **67**, 054017 (2003) [arXiv:hep-ph/0210045].

[40] M. Diehl and P. Kroll, Phys. Lett. B **683**, 165 (2010) [arXiv:0911.3317 [hep-ph]].

[41] S. Uehara *et al.* [Belle Collaboration], Phys. Rev. D **80**, 032001 (2009) [arXiv:0906.1464 [hep-ex]].

[42] T. Feldmann and P. Kroll, Phys. Lett. B **413**, 410 (1997) [arXiv:hep-ph/9709203].

[43] M. Wirbel, B. Stech and M. Bauer, Z. Phys. C **29**, 637 (1985).

[44] G. T. Bodwin, E. Braaten and G. P. Lepage, Phys. Rev. D **51**, 1125 (1995) [Erratum-ibid. D **55**, 5853 (1997)] [arXiv: hep-ph/9407339].

[45] R. Barbieri, E. d'Emilio, G. Curci and E. Remiddi, Nucl. Phys. B **154**, 535 (1979).

[46] M. A. Shifman amd M. I. Vysotskii, Nucl. Phys. B **186**, 475 (1981).

[47] J. P. Lansberg and T. N. Pham, Phys. Rev. D **74**, 034001 (2006) [arXiv:hep-ph/0603113].

[48] K. Nakamura *et al.* [Particle Data Group], JPG **37**, 075021 (2010).

[49] S. Ong, Phys. Rev. D **52**, 3111 (1995).

[50] M. Diehl, P. Kroll and C. Vogt, Eur. Phys. J. C **22**, 439 (2001) [arXiv:hep-ph/0108220].

[51] B. Melic, D. Mueller and K. Passek-Kumericki, Phys. Rev. D **68**, 014013 (2003) [arXiv:hep-ph/0212346].

[52] P. Kessler and S. Ong, Phys. Rev. D**48**, 944 (1993).

[53] J.M. Cornwall, Phys. Rev. Lett. **16**, 1174 (1966); G. Köpp, T.F. Walsh and P. Zerwas, Nucl. Phys. B **70**, 461 (1974).

[54] B. Aubert *et al.* [The BABAR Collaboration], Phys. Rev. D **74**, 012002 (2006) [arXiv:hep-ex/0605018].

[55] T. Gousset and B. Pire, Phys. Rev. D **51**, 15 (1995) [arXiv:hep-ph/9403293].

[56] L. Magnea and G. Sterman, Phys. Rev. D **42**, 4222 (1990).

[57] I.V. Musatov and A.V. Radysuhkin, Phys. Rev. D **56**, 2713 (1997) [arXiv:hep-ph/9702443].

[58] N. G. Stefanis, W. Schroers and H. C. Kim, Eur. Phys. J. C **18**, 137 (2000) [arXiv:hep-ph/0005218].

[59] J. Bolz, PhD thesis (WUB-DIS 95-10), Universität Wuppertal, 1995, in German, quoted in M. Dahm, R. Jakob and P. Kroll, Z. Phys. C **68**, 595 (1995) [arXiv:hep-ph/9503418].

[60] S. Descotes-Genon and C. T. Sachrajda, Nucl. Phys. B **625**, 239 (2002) [arXiv:hep-ph/0109260].

[61] D. E. Soper, Nucl. Phys. B **163**, 93 (1980).

[62] G. M. Huber *et al.* [Jefferson Lab Collaboration], Phys. Rev. C **78**, 045203 (2008) [arXiv:0809.3052 [nucl-ex]].